Forest Ecology and Management 473 (2020) 118308

Contents lists available at ScienceDirect

Forest Ecology and Management

journal homepage: www.elsevier.com/locate/foreco

Small gradients in salinity have large effects on stand water use in freshwater wetland forests

Jamie A. Duberstein[a,*], Ken W. Krauss[b], Michael J. Baldwin[b], Scott T. Allen[c,d], William H. Conner[a], John S. Salter Jr.[a], Michael Miloshis[e]

[a] Clemson University, Baruch Institute of Coastal Ecology and Forest Science, Georgetown, SC, USA
[b] U.S. Geological Survey, Wetland and Aquatic Research Center, Lafayette, LA, USA
[c] Louisiana State University, School of Renewal Natural Resources, Baton Rouge, LA, USA
[d] University of Utah, Geology and Geophysics Department, Salt Lake City, UT, USA
[e] Charles Darwin University, College of Engineering, IT & Environment, Darwin, Northern Territory, Australia

ARTICLE INFO

Keywords:
Wetlands
Baldcypress
Water tupelo
Sap flow
Salinity
Ecohydrology

ABSTRACT

Salinity intrusion is responsible for changes to freshwater wetland watersheds globally, but little is known about how wetland water budgets might be influenced by small increments in salinity. We studied a forested wetland in South Carolina, USA, and installed sap flow probes on 72 trees/shrubs along a salinity gradient. Species investigated included the trees baldcypress (*Taxodium distichum* [L.] Rich.), water tupelo (*Nyssa aquatica* L.), swamp tupelo (*Nyssa biflora* Walt.), and the shrub waxmyrtle (*Morella cerifera* (L.) Small). This study improves upon past reliance on greenhouse seedling studies by adding measurements of trees/shrubs along a salinity gradient, and better describes the role of low salinity on water use in freshwater wetland forests. We measured patterns of water use related to salinity, atmospheric conditions and season, and hypothesized that salinity would influence wetland forest water use through two mechanisms: salinity disturbances would yield stands with species and size classes that transpire less and individual trees with less conductive xylem tissue (i.e., sapwood). Both hypotheses held. At salinity concentrations ranging from fresh to 3 psu, forest structural changes alone resulted in stand water use reductions from 494 mm year^{-1} in freshwater stands to 316 mm year^{-1} in stands of slightly higher salinity. Tree sapwood function (inferred from radial sap flux profiles) also changed along this gradient and reduced sap flow rates by an additional 13.3% per unit increase in salinity (psu). Thus, stand water use was further reduced to 190 mm year^{-1} on saline sites. We found that forest structure is not the only change that affects water use in salinized watersheds; individual tree eco-physiological responses to salinity, manifesting in different radial sap flow profiles, are important as well.

1. Introduction

Wetland forests in coastal areas undergo episodic pulses of salinity. The salinity can come from a number of different sources, including storm surges (Michener et al., 1997; Conner et al., 1997), sea-level rise (Williams et al., 1999), and human environmental modification associated with land use change, river damming, dredging of navigation corridors, and the landward intrusion of saline groundwater due to pumping, as well as hydrocarbon extraction (Salinas et al., 1986; Ericson et al., 2006; Day et al., 2007). In the Southeastern United States, saltwater intrusion into freshwater wetlands has led to changes in the distribution of specific habitats throughout the Holocene (Jones et al., 2017), such that natural processes drove the alternation between forests and marsh, even before humans strongly influenced the landscape. In fact, William Bartram, traveling in what is now present-day Florida, USA, remarked in his *Travels* (circa 1791) that "…salt marshes adjoining the coast of the main, and the reedy and grassy islands and marshes in the rivers, which are now overflowed at every tide, were formerly high swamps of firm land, affording forests of Cypress, Tupilo [*sic*], …, the same as are now growing on the river swamps, whose surface is two feet or more above the spring tides…" (p. 79; Van Doren, 1928). Bartram described a sea-level rise mediated transition that eventually resulted in more permanent salinization, thus influencing transition from forest to marsh by, in part, affecting the way trees first adapted to salinity and then died.

This transition from fresh to saline water results in physiological

---

* Corresponding author.
E-mail address: jdubers@clemson.edu (J.A. Duberstein).

https://doi.org/10.1016/j.foreco.2020.118308
Received 2 February 2020; Received in revised form 3 June 2020; Accepted 4 June 2020
Available online 25 June 2020
0378-1127/ © 2020 Elsevier B.V. All rights reserved.

and structural changes that may affect stand water use by influencing salinity-imposed soil osmotic gradients (Carter et al., 2006a) and forcing trees to take up greater concentrations of Na^+ and Cl^- during transpiration (Yanosky et al., 1995). Such changes in tree- and stand-level transpiration may substantially influence local hydrology. However, to date, insights into how wetland forest water use is influenced by environmental stress related to sea-level rise and saltwater intrusion are heavily based on seedling studies in controlled settings. While useful, these studies provide inadequate tools to predict hydrologic changes in the field and at the scales of interest to water resource managers. Fortunately, efforts to pair sap flow and modeling with environmental variables to determine stand water use and evapotranspiration (ET) in forests have become routine in water resources research (e.g., Čermák et al., 1995; McLaughlin et al., 2012; Tie et al., 2018; etc.). Yet, few studies have used sap flow measurements to specifically understand the influence of long-term salinity stress on tree or stand water use. Such studies are needed to understand the impact of salinization on forested wetland water budgets.

Wetland trees may be inherently conservative in water use compared to their upland counterparts, especially when exposed to salinity. Salinity imposes less favorable soil osmotic conditions for plant water extraction (Munns and Termaat, 1986), and this can influence individual tree size class/leaf area distribution and internal sapwood function in low-salinity adapted wetland forests (Krauss and Duberstein, 2010). Wullschleger et al. (1998) reviewed individual tree water use data from 52 species of upland trees and found seven species who used 300–530 L H_2O day^{-1} and one species found in the Amazon rainforest that used 1180 L H_2O day^{-1}; most reports indicated water use of mature trees up to 200 L H_2O day^{-1}. In comparison, individual baldcypress (*Taxodium distichum* [L.] Rich.) trees used 100 L H_2O day^{-1} in relatively freshwater environments (<1 psu salinity), but only 24 L H_2O day^{-1} when exposed to chronic salinity (up to 5.5 psu salinity during a drought) despite similar stand ages and continuous water availability at both sites (Krauss and Duberstein, 2010). With few previous studies, we have little conceptual understanding of how salinity influences the wetland-forest water balances along other salinity gradients. We therefore ask whether changes in stand water use can be predicted from salinity-imposed forest structural changes alone, or if the physiological effects of salinity on individual trees must also be considered.

Individual tree and stand water use estimation requires some assumptions and steps. First, it has been shown that rates of sapflux vary with radial depth into the sapwood for many tree species (e.g., Phillips et al., 1996; James et al., 2003; Ford et al., 2004; Poyatos et al., 2007; and others), and that radial depth partitioning can vary with salinity (Krauss and Duberstein, 2010). Therefore, it is not sufficient to simply insert a probe at a specific depth in low and high salinity environments and compare rates of sap flow to determine differences in individual tree water use. The measurements need to be scaled to account for variability in flow rates at different radial depths. For example, the majority of sapflux in baldcypress growing in a salinity-impacted environment (albeit low; 5 psu) occurred at very shallow radial depths (1.5 cm) in contrast to much higher rates of water use (approximately twice as much) at 2.5 cm radial depths in trees growing in a freshwater environment (Krauss and Duberstein, 2010).

Second, in situ studies to determine stand water use require careful consideration of many factors in order to make meaningful conclusions. For example, only 4–6 forest plots (0.05 ha each) would be required to discern differences for stands that differ by 500–600 mm H_2O $year^{-1}$ due to variability in plot level stand water use calculations. However, for forest stands that differ in water use by <350 mm H_2O $year^{-1}$, >12 plots may be required (Krauss et al., 2015a), and it would be both difficult and expensive to instrument that many plots with sap flow sensors. Furthermore, it is a challenge to control for salinity (or any environmental stress) between two sites properly because they could differ in other environmental factors (e.g., soil structure, fertility, hydroperiod, etc.), and differences could scale non-linearly as one transgresses between sites. Our study site offered a unique opportunity to investigate the effects of forest structure and salinity within a relatively short distance (250 m), aided greatly by a previously established boardwalk by which we could access our deployed equipment.

While past studies led us to expect that freshwater wetland forests experiencing extended durations of low salinity (≤ 3.5 psu) will have lower total water use, here we evaluate two hypotheses on how differences might manifest. First, individual trees in increasingly saline environments will have different radial water patterning leading to overall lower individual tree water use. Here, we use a gradient experimental design (sensu Ellis and Schneider, 1997) to incorporate a range of tree species, characterize sap flow for those species at different salinities, and develop a sense for changes in water use by the dominant wetland forests occurring along gradients of salinity in Southeastern U.S. watersheds. Second, optimal growing conditions in the freshwater sites leads to larger and more densely packed trees and thus higher water use. If this is true, lower total water use in saline forests may be the result of the combined factors of lower conductance through the radial profile and lower total basal area.

2. Methods

2.1. Study site

Strawberry Swamp is located on Hobcaw Barony, which is approximately 7 km east of Georgetown, South Carolina, USA (33°19′49″N, 79°14′54″W), just bordering Winyah Bay along the Atlantic Ocean (Fig. 1). Hobcaw Barony incorporates approximately 6800 ha of managed pine forest interspersed with several distinctive transitions between uplands and salt marshes that include a number of freshwater wetland forests. Many of these wetland forests were historically tidal but were logged in the late 1700′s during colonial land development and allowed to regenerate into their current structure naturally over time. Their hydrology was managed to remain relatively fresh in order to serve as reservoirs for coastal rice cultivation (Smith, 2012). Rice fields were seaward of reservoirs, and the reservoirs were used for flushing salinity from rice fields. The Civil War (1861–1865) abruptly changed this practice, and many coastal reservoir and rice sites were abandoned, with some areas returning to tidal wetlands as levees and water control structures deteriorated. Strawberry Swamp represents one of these reservoir sites, though it periodically receives pulses of salinity.

A significant pulse of salinity resulted from Hurricane Hugo in 1989, but the primary source of contemporary and consistent salinity into Strawberry Swamp may instead be related to flow reversals coincident with low river flows, primarily the Pee Dee River, into the adjacent Winyah Bay, as occurred during perennial drought conditions in the early 1980s, early 1990s, and 2002–2005 (Williams et al., 2012; T.M. Williams, pers. comm.). Currently, Strawberry Swamp occupies 236 ha (Fig. 1), is permanently flooded and has a unique characteristic in that it has very little water level fluctuation over time (long hydroperiod). This study site is unique because the upland freshwater influence in this hydrologically enclosed landscape promotes a sharp contrast in salinity over a relatively small range (3 psu over approximately 250 m).

Dominant tree species of Strawberry Swamp and the Hobcaw Barony wetland forests include baldcypress, water tupelo (*Nyssa aquatica* L.), swamp tupelo (*Nyssa biflora* Walt.), green ash (*Fraxinus pennsylvanica* Marsh.), red maple (*Acer rubrum* L.), and sweet gum (*Liquidambar styraciflua* L.). These are all deciduous trees well-adapted to freshwater conditions. Evergreen loblolly pine (*Pinus taeda* L.) may occasionally be found in these wetlands at slightly higher microtopographic elevations. Shrub species include dahoon (*Ilex cassine* L.) and waxmyrtle (*Morella cerifera* (L.) Small), and just at the transition between wetland forest and marsh at Strawberry Swamp, the common reed (*Phragmites australis* (Cav.) Trin. Ex Steud.) begins to dominate the

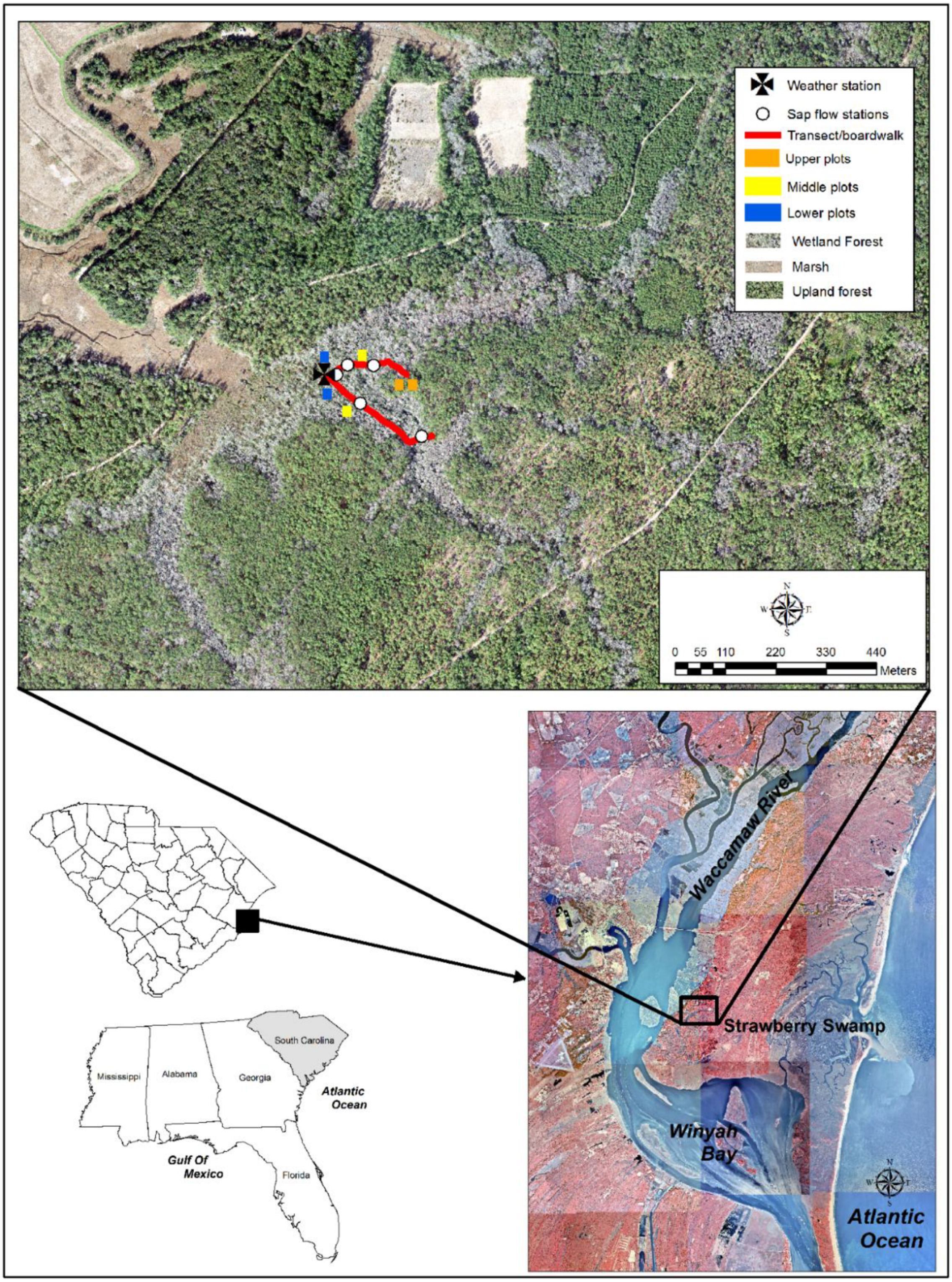

Fig. 1. Location of Strawberry Swamp (depicted as "Wetland Forest") along the Atlantic Coast of South Carolina, USA, at Hobcaw Barony, showing adjacent land uses and our two study transects (gradients) along boardwalks (red lines each ending at cross), which span from upland forest to marsh and converge at an apex (cross symbol). The location of the five sap flow stations is depicted as white dots along these two transects. From these stations, cables were run to overlapping individual trees along the gradient, and 20 salinity wells (not shown here) were dispersed along these transects and associated with those individual trees. Image was taken in the winter, showing a color contrast among the locations of deciduous wetland forest, senescent marsh, and evergreen upland forest. (For interpretation of the references to color in this figure legend, the reader is referred to the web version of this article.)

understory. Other marsh species include big cordgrass (*Spartina cynosuroides* (L.) Roth), sturdy bulrush (*Bolboschoenus robustus* (Pursh) Sojak), and cattail (*Typha* L.).

2.2. Forest plots and transects

We used two overlapping experimental designs at Strawberry Swamp, one to measure forest structure and the other to measure sap flow (Fig. 1). First, forest plots and survey techniques for trees ≥ 10 cm diameter at breast height (*dbh*) were established at Strawberry Swamp using six, 20 × 25-m plots, with two each in upper, freshwater locations (0.7 psu), and two each in both higher salinity middle (2.6 psu) and lower (3.0 psu) stand locations closer to the estuary and source of salinity (Liu et al., 2017). These plot-based forest structural data were used to describe the transition from upland to marsh at discrete points using standard forestry metrics, and were later used to determine stand water use based on those forestry metrics (see below). Second, two transects representing the same salinity gradient from the upland forest edge to marsh were established. Five sap flow stations were set up along these transects (Fig. 1), and cables (up to 30 m long) were run to provide near-continuous coverage along the salinity gradient, and overlapping the forest plots. We installed thermal dissipation sap probes on 72 trees along this low salinity gradient of 0.3 to 3.3 psu (i.e., much lower than the 35 psu of full-strength sea water).

By design, the location of the forest plots did not constrain our measurements of sap flow and salinity along the gradient. We focused our forest plot measurements on surveying all species within the plots, and we focused the sap flow assessment on specific dominant species, comprising baldcypress, water tupelo, swamp tupelo, and waxmyrtle. These species made up 92–99% of total basal area in Strawberry Swamp (Table 1). Soils at Strawberry Swamp include highly organic layers overlying moderately fine silicates, characterized as fine-loamy, siliceous, thermic, Typic Umbraquults (Stuckey, 1982).

Table 1
Characteristics of canopy tree species (*dbh* $\geq$ 10 cm) for three stand conditions along a salinity gradient at Strawberry Swamp, Hobcaw Barony, South Carolina, USA.

Stand	Salinity (psu)[a]	Canopy species[b]	Stem density (stems ha^{-1})	Basal area (m^2 ha^{-1})	Average *dbh* (cm)
Upper	0.7 ± 0.4	baldcypress	290	23.9	28.2
		swamp tupelo	250	13.4	24.7
		water tupelo	140	16.7	37.0
		ash spp.	60	3.6	25.6
		sweetgum	50	0.9	14.8
		dahoon	10	0.2	14.1
		Total	**800**	**58.6**	–
Middle	2.6 ± 0.9	baldcypress	260	43.6	44.9
		swamp tupelo	170	5.9	20.3
		water tupelo	140	15.5	34.7
		waxmyrtle	30	0.4	12.2
		red maple	10	0.4	23.0
		loblolly pine	10	0.1	11.6
		Total	**620**	**65.9**	–
Lower	3.0 ± 1.0	baldcypress	250	47.4	47.7
		water tupelo	120	6.6	24.1
		swamp tupelo	130	3.5	17.6
		waxmyrtle	60	0.7	11.7
		ash spp.	10	0.1	10.5
		loblolly pine	10	0.1	10.9
		Total	**570**	**58.3**	–

[a] Salinity values differ from Liu et al. (2017) in that we assessed wells with greater spatial and temporal rigor to coincide with sap flow measurements (see text).

[b] Baldcypress (*Taxodium distichum*), swamp tupelo (*Nyssa biflora*), water tupelo (*Nyssa aquatica*), ash (*Fraxinus* sp.), sweetgum (*Liquidambar styraciflua*), dahoon (*Ilex cassine*), waxmyrtle (*Morella cerifera*), red maple (*Acer rubrum*), loblolly pine (*Pinus taeda*).

2.3. Environmental measurements

Salinity was previously reported for forest plots in Liu et al. (2017), but those data are updated here. A total of 20 monitoring stations were installed within 1.2–16.8 m (median = 5.1 m) of each tree being measured for sap flow along the transects, and salinity measurements were related to those specific trees. Salinity monitoring stations included two wells so that measurements could be taken at two sampling depths, shallow (6.5–20 cm) and deep (60–100 cm), allowing us the ability to assess the additional objection of discerning which depth (of measured salinity) influences sap flow more. Salinity measurements were taken weekly using a hand-held meter (model 30, YSI Inc., Yellow Springs, OH, U.S.). Groundwater levels were measured continuously in three wells (model CTD-10, Decagon, Pullman, WA, U.S.). Air temperature (T) and relative humidity (RH) were measured 7.5 m above the soil surface from a tower deployed just at the transition (canopy clearing) between forest and marsh (location depicted by the cross symbol, Fig. 1) using a combination probe (model HMP45C, Vaisala, Helsinki, Finland). T and RH data were used to calculate vapor pressure deficit (D). Photosynthetic Photon Flux Density (PPFD) was measured from a position unobscured by the canopy at that same tower height using a base-leveled quantum sensor (model Li-190SA, Li-Cor Environmental, Inc., Lincoln, NE, U.S.). All data were recorded at 15-min intervals using a data logger (model CR800, Campbell Scientific, Inc., Logan, UT, U.S.).

Potential evapotranspiration (PET) was estimated at the site as a function of available energy (net radiation plus the ground heat flux); although this is a metric of PET, we assume it also serves as a proxy for actual ET in this environment of excess water. Net radiation was measured from the same tower but at a 14 m height with a net radiometer (model NR-lite2, Kipp Zonen, Delft, Netherlands). Ground heat flux was estimated using water level and water temperature profile measurements (<5 cm below the water surface, 20 cm above the soil water surface, at the soil–water interface, and 20 cm below the soil surface) to calculate changes in stored heat, following the method described in Allen et al. (2017). With these data, equilibrium evaporation was calculated and then adjusted by an assumed factor of 1.26 (Priestley and Taylor, 1972), which is a reasonable estimate of PET in expansive, wet regions (De Bruin and Keijman, 1979). Gaps in the above-canopy data series were estimated as a function of solar radiation measured at an independent meteorological station (National Estuarine Research Reserve System, https://cdmo.baruch.sc.edu/) approximately 5.28 km from the research site, and understory net radiation measured with a net radiometer (RMSE = 0.7 mm day^{-1} for PET). PET was calculated on a 1-day time step using smoothed 7-day running mean input data, to show the seasonal progression of PET relative to that of transpiration.

2.4. Sap flow measurements and stand water use

We used thermal dissipation probes (TDP) (models TDP 10–100, Dynamax, Inc., Houston, TX, USA) to measure sap flow in the four tree species at variable radial depths of 5, 15, 25, 50, 70, and 90 mm into the sapwood using installation procedures that were outlined previously from other wetland forests (Duberstein et al., 2013). Probes were installed at acceptable heights for these species (e.g., above buttress) on the north side of the trees for consistency and were shielded with reflective insulation material. We did not measure the hypothetical effects of probe azimuth on sap flow rates because of data logger channel restrictions, but we recognize that for at least one species, baldcypress, consistent sap flow measurement on the north side led to some bias at a site in North Carolina, U.S. (Oren et al., 1999).

A total of 72 trees were instrumented along the Strawberry Swamp salinity gradient: 36 baldcypress, 21 water tupelo, 13 waxmyrtle, and 2 swamp tupelo. Sap flow data were recorded every 30 min simultaneously on five data loggers (model CR1000, Campbell Scientific, Inc.,

Table 2
Number of thermal dissipation probes deployed at various depths (of thermocouples: TC) inside the cambium, and the corresponding width of bands of active xylem to which the attenuation functions were applied during modeling.

TC Depth (mm)	# Probes	Xylem Band (mm)
5	8	0 – 10[a]
15	66	0 – 20[b]
25	16	20–40
50	16	40–60
70	16	60–80
90	16	80–100

[a] Waxmyrtle only.
[b] Waxmyrtle xylem band was 10–40 mm.

Logan, UT, USA) spanning a distance of 230 m to include the full salinity gradient (Fig. 1; single data logger present at each of the "sap flow stations"). All trees were in the co-dominant crown class, except for waxmyrtle, which is an understory shrub that progressively advances to greater relative dominance as salinity increases along the gradient. In all, 8 sap flow measurement probes were established at radial depths of 5 mm (waxmyrtle only), 66 sap flow measurement probes were established at radial depths of 15 mm, and 16 sap flow measurement probes each were established at radial depths of 25, 50, 70, and 90 mm, for a total of 138 continuously logging probe pairs (Table 2). Several trees were used for multiple depth measurements to account as comprehensively as possible for radial variation in sap flow within the sapwood of sample trees.

Temperature differences between paired heated and unheated probe sets were collected from 25 April to 24 September 2015. Data are available from ScienceBase (Duberstein et al., 2018). Data were organized by species, probe pair, and radial depth, and used to determine sap flow rates in grams (g) H_2O m^{-2} s^{-1} using formulation, procedures, and assumptions previously described (Granier, 1987; Clearwater et al., 1999; Lu et al., 2004; Krauss et al., 2015a). No-flow periods for calculations were determined between 0100 and 0600 each morning and applied newly each day. While sustained night-time sap flow and possible transpiration were not discernable using our approach (i.e., no flow between 0100 and 0600), water movement persisted within the stems of many of the trees until midnight on many evenings, which may indicate some water loss that would have been unquantifiable through our approaches (Dawson et al., 2007). However, the diurnal sap flux patterns did not vary in obvious ways along the salinity gradient. Furthermore, in this humid environment, night-time *D*, the gradient driving transpirational fluxes, is small.

Individual tree water use (L H_2O day^{-1}) and stand water use (mm H_2O day^{-1}) were determined through calculation and modeling procedures described in much greater detail in previous papers (Krauss et al., 2015a, 2015b). In short, the modeling procedure uses average maximum sap flow rates by species recorded from a range of days with high *D* and no rainfall, and then sap flow is scaled using radial attenuation functions developed on-site and applied to corresponding functional sapwood area of individual trees modeled. This establishes instantaneous maximum water use of an individual tree (L H_20 s^{-1}). Instantaneous maximum water use values are then scaled to maximum daily integrated sap flow rates using 30-min-resolution relative sap flow response by time interval and species from those same high *D* days used to establish average maximum sap flow. This yields maximum individual tree water use per species per day (L H_2O day^{-1}) under high *D* conditions. Forest plot-based *dbh* data are then used to determine plot-scale water use, which is further adjusted to the area of the plot to determine maximum potential daily water use (kg H_2O m^{-2} of ground area, or mm). Plot-scale daily water use rates are then adjusted to annual rates using daily integrated *D*. These are not scaled base on a simple proportion such that a 10% lower cumulative D results in 10% lower water use. Rather, they are based on diurnal attenuation functions developed as a percent attenuation for each 30-minute interval during the days selected as having maximum *D* (Krauss et al., 2015a). Separate diurnal functions were developed for baldcypress and waxmyrtle, though water tupelo and swamp tupelo were both modeled from data derived from water tupelo due to the lower number of study trees. We assume maximum plot-scale daily water use rates occurred on the day with the highest *D*, and are hindcasted to additional individual days using the diurnal attenuation functions and PPFD (Krauss et al., 2015a). The diurnal constant is applied to all days throughout the year, although annual shifts in diurnal light yields do occur.

For tree species included in Strawberry Swamp forest survey plots, but not directly assessed for sap flow in this study, we used sap flow data measured at a nearby site (Bannockburn Plantation; Krauss et al., 2015a); these species included ash (*Fraxinus* sp.), sweetgum, red maple, and loblolly pine, collectively comprising a very small percentage of stand water use at Strawberry Swamp. Because we initiated the sap flow study in April when many trees had just initiated bud growth and were actively transpiring, annual patterns of sap flow initiation for Strawberry Swamp were estimated using data from the same nearby site. Annual patterns of sap flow cessation were measured directly from Strawberry Swamp. For example, sap flow for baldcypress started decreasing in mid-October and was not completed until the end of November, while sap flow in *Nyssa* spp. was completed entirely by September.

2.5. Statistical analyses

We hypothesized that differences in salinity influence stand water use through two primary mechanisms: (1) by altering how individual trees of similar size use water, and (2) by changing forest structure to more sparsely structured wetland forests with larger trees. For Hypothesis 1, we used different regression analyses to determine the response of individual tree eco-physiology (i.e., patterning radial fluxes) to the influence of salinity. In order to determine how differences in water use are manifested to changes in forest structure (Hypothesis 2), stand water use was modelled using tree diameter distributions by species from the forest survey plots (N = 2 plots each in upper, middle, and lower stand locations), ignoring any influence of salinity on tree-level sap flow. Changes in output were the result of survey plot-level forest structural changes along the salinity gradient only. We then applied the corrections to the additively to the stand water use data generated by testing Hypothesis 2. To do this, we first developed a series of regressions that would account for the influence of salinity for each radial sapwood depth (5, 15, 25, 50, 70, 90 mm) for each applicable species. Our gradient design does not identify the specific location along the salinity gradient where radial patterning begins to shift and influence water use. Therefore, and second, we ran a linear regression model with an autoregressive (AR) error of sap flow on salinity (measured weekly) by species (baldcypress, water tupelo, waxmyrtle) which assesses the independent variable (sap flow) along two dependent variable axes (salinity, radial depth) simultaneously to develop predictive equations. This procedure allows an inherent treatment of both sap flow and radial depth variation in sap flow of trees as salinities increased along the continuous gradient dynamically through the study period.

Individual and overall regression models of radial fluxes as a function of salinity were tested for homogeneity of residual variance and normality; no transformations were needed. Differences in individual tree water use characteristics by species were determined using a two-way ANOVA after data were square-root-transformed to achieve normality and variance equality. These analyses were conducted with SAS 9.4 Software (SAS Institute Inc., Cary, North Carolina, U.S.).

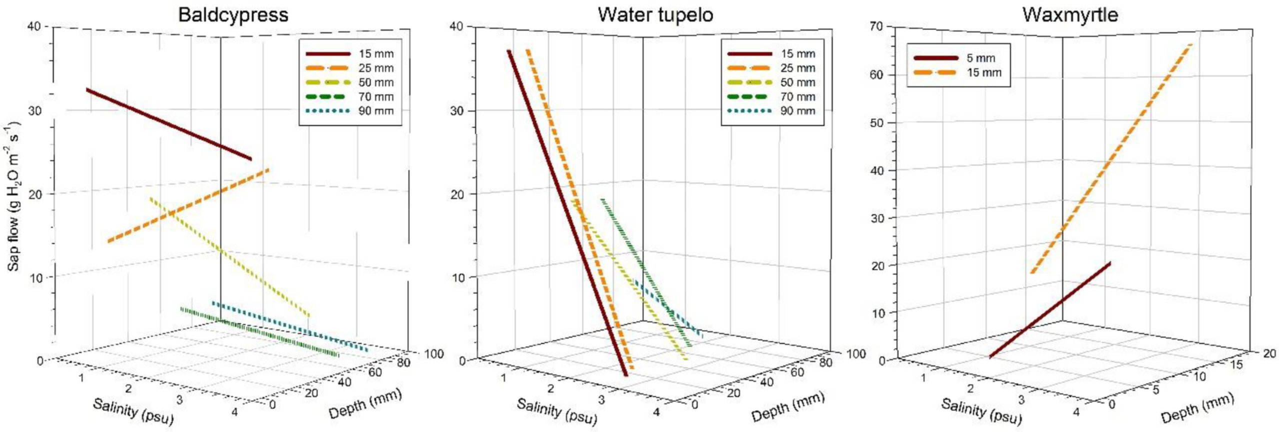

Fig. 2. 3-D depiction of sap flow for all species (baldcypress, water tupelo, waxmyrtle) by radial sapwood depth (15, 25, 50, 70, 90 mm) and salinity (0–4 psu) for co-dominant trees associated with a salinity gradient at Strawberry Swamp, Hobcaw Barony, South Carolina, USA.

3. Results

3.1. Salinity and sap flow rates by radial depth

Salinity conditions in shallow and deep wells in Strawberry Swamp did not vary considerably through the study period for most sample locations (n = 18 well locations) with an average difference of salinity (i.e., maximum–minimum measured) of 1.1 ± 0.2 psu for all wells (n = 36). The greatest variability in salinity was at lower stand positions (avg. 1.7 ± 0.5 psu) where salinities were consistently highest, trees larger and more sparse (Table 1), waxmyrtle more abundant, and common reed becoming established; the maximum difference in salinity was 2.7 psu measured in a deep well in this area.

Maximum daily sap flow rates (i.e., on high *D* days) were correlated with salinity at two separate soil depths. Sap flow rates were slightly more strongly associated with porewater salinity measured from deeper soil depths of 60–100 cm ($0.11 < r^2 < 0.73$) than from shallower soil depths of 6.5–20 cm ($0.01 < r^2 < 0.64$), potentially indicating that sap flow in the trees might be more sensitive to salinity of deeper porewater. Furthermore, sap flow of baldcypress and water tupelo versus salinity generally pointed to an inverse relationship between salinity and sap flow for radial sapwood depths of 15, 25, 50, 70, and 90 mm (Fig. 2). The *x*-intercepts (i.e., salinity concentrations at which sap flow becomes zero) for these radial depths generally ranged from 1.05 to 5.18 psu (but with one apparent outlier at 14.55 psu), and only 2 of 12 species and depth combinations had no intercept that could be inferred (Table 3). The significance of these univariate regressions was also variable, with only 3 of the 12 combinations being significant (at $P \leq 0.05$) when explored in this fashion.

Table 3
Statistical summary of sap flow reduction by species for various radial depths into the sapwood for co-dominant trees associated with a salinity gradient at Strawberry Swamp, Hobcaw Barony, South Carolina, USA.

Species[a]	Radial depth (mm)	*x*-intercept, salinity (psu)	*y*-intercept, sap flow (g H_2O m^{-2} s^{-1})	r^2	Pr > F
baldcypress	15	14.552	32.772	0.106	0.053
	25	Undefined	13.106	0.275	0.120
	50	5.184	18.979	0.225	0.166
	70	4.065	3.175	0.728	0.007
	90	3.596	3.200	0.328	0.083
water tupelo[b]	15	2.606	38.891	0.295	0.016
	25	2.370	39.467	0.253	0.309
	50	2.622	19.205	0.306	0.255
	70	2.064	18.816	0.677	0.012
	90	1.706	6.663	0.308	0.253
waxmyrtle	5	1.052	Undefined	0.108	0.426
	15	Undefined	11.270	0.452	0.098

[a] Baldcypress (*Taxodium distichum*), water tupelo (*Nyssa aquatica*), and waxmyrtle (*Morella cerifera*).

[b] Relationships also used for swamp tupelo (*Nyssa biflora*) in our analyses.

Indeed, the effect of the salinity gradient on sap flow differed by species. Baldcypress sap flow mostly declined with higher salinity, but only slightly as salinities ranged from 0.7 to 3.0 psu (Fig. 2). Water tupelo sap flow declined strongly along the salinity gradient; no water tupelo trees were present at salinities >2.2 psu in Strawberry Swamp. The effects of salinity on water use in waxmyrtle is less variable than for baldcypress and water tupelo. Regressions describing the sap flow response along the salinity gradient for radial sapwood depths of 5 mm and 15 mm were not significant ($r^2 = 0.11–0.45$; $P = 0.098–0.426$) but tended to increase with salinity (Fig. 2; Table 3). However, this relation was confounded by progressively greater light levels to mid-story canopies as salinity increased, preventing an assessment of salinity alone for waxmyrtle.

While the response of sap flow at depth are best described as linear functions, it is important to point out that these relationships were derived through non-linear analysis of the empirical data. Once the combined salinity and depth relationships were established (Fig. 2, Table 3), multiplier functions (Fig. 3) were applied in the stand water use modeling procedure – first without salinity in the model itself, and then with salinity. These salinity-adjusted multipliers describe the sapwood area scaled attenuation of sap flow with depth into tree. The multipliers were applied to areas of active xylem that were based on bands corresponding to radial depth measurements. For example, radial depth measurements at 15, 25, and 50 mm were used for multipliers applied to bands of active xylem of 0–20 mm, 20–40 mm, and 40–60 mm, respectively (see Krauss et al., 2015a, 2015b). This modeling procedure allowed us to apply the multipliers, which incorporate radial depth and salinity, to individual tree sapwood areas in a weighted fashion based on *dbh*.

3.2. Stand water use in the absence of salinity

To model stand water use of the freshwater wetland forest at Strawberry Swamp, it was first critical to determine average maximum rates of sap flow for all species growing in Strawberry Swamp. The average maximum rate of sap flow for baldcypress was 35.85 g H_2O m^{-2} s^{-1} (n = 36 trees), for water tupelo was 46.04 g H_2O m^{-2} s^{-1} (n = 19 trees), for swamp tupelo was 86.26 g H_2O m^{-2} s^{-1} (n = 2 trees), and for waxmyrtle was 50.89 g H_2O m^{-2} s^{-1} (n = 7 trees). These rates were derived from the five study days with the highest

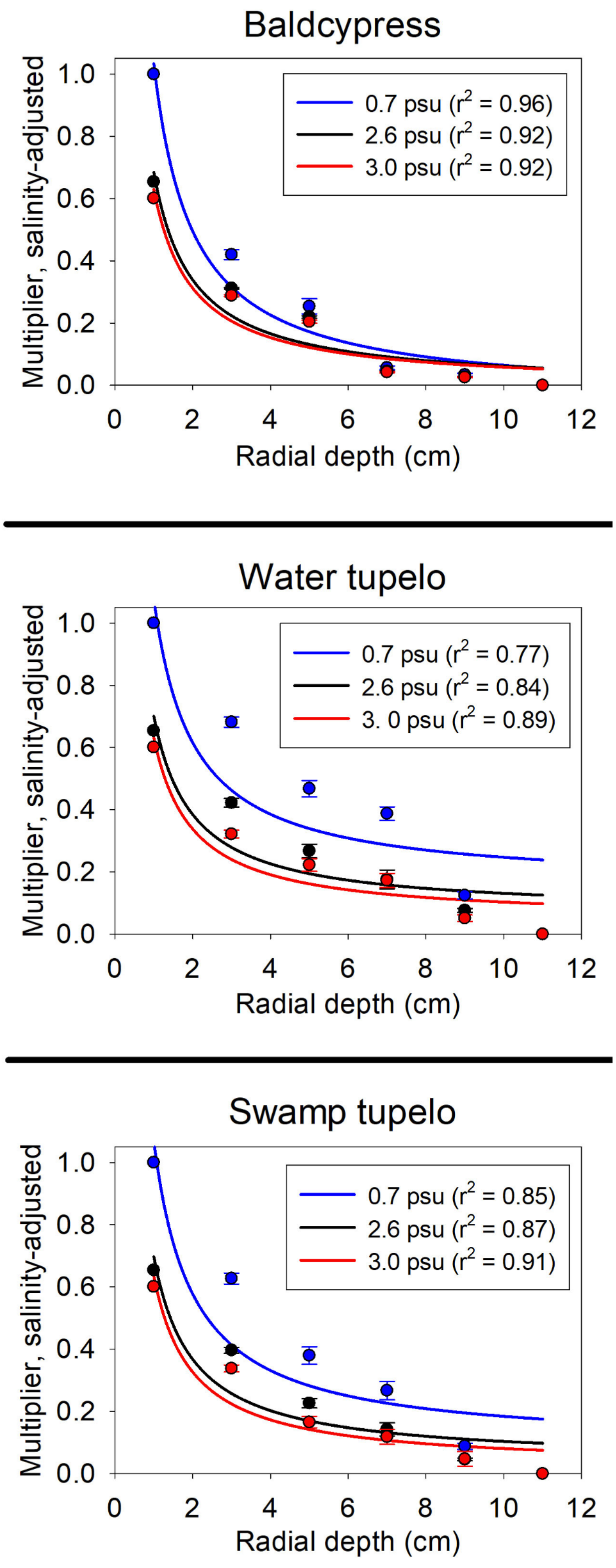

Fig. 3. Regressions of stand water use multipliers, which combine forest structure suppression and salinity suppression, versus radial depth into the xylem of three tree species in Strawberry Swamp.

maximum D (at 3.42–4.49 KPa), and differ from those values reported in Table 3 in that only trees growing under freshwater conditions were used to determine maximum sap flow rates for baldcypress and water tupelo. A summary of the average daily maximum for all four species across the entire range of usable data ($n = 63$ days, all without rain events) is provided in Table S1. The average maximum daily flow rates for individual trees is provided in Table S2. Stand water use modelling assumes suppression of sap flow on days with lower D relative to maximum rates observed at the highest D. Swamp tupelo and waxmyrtle measurements were taken from trees growing in only slightly higher salinities, which is where they happen to occur within Strawberry Swamp.

Among locations that remained < 1 psu salinity over the course of study, the radial attenuation of sap flow with depth into the sapwood was greater for baldcypress for all depths relative to water tupelo (data not shown). Sap flow for baldcypress was especially suppressed at depths beyond 50 mm, which means that they had effectively less cross-sectional area of conductive tissue per basal area, even under freshwater conditions, relative to the other species at Strawberry Swamp. Daily rates of stand water use in freshwater portions of Strawberry Swamp follow estimated potential evapotranspiration (Fig. 4). On an annual basis, stand water use for the freshwater stands at Strawberry Swamp was estimated to be 494 mm H_2O year^{-1}, with most water use associated with the deciduous, dominant tree species baldcypress, water tupelo, and swamp tupelo. Water use estimation from the two plots located within the upper, freshwater stands differed by only 8 mm H_2O year^{-1} between them, with evergreen trees comprising $< 1.2\%$ of that water use (Table 4).

3.3. *Stand water use in the presence of salinity*

The largest individual trees in the middle and lower stands were baldcypress (Table 1). The sizes and densities of the other tree species were lower in those plots, supporting the potential of baldcypress to have a dominant influence on stand water in that area of higher salinity. These changes in forest structural characteristics (ignoring the effects of the salinity on tree-level sap flow rates) are responsible for a difference in stand water use of 494 mm H_2O year^{-1} in freshwater stands (at 0.7 ± 0.4 psu; mean ± S.D.) to 393 mm H_2O year^{-1} in middle stands (at 2.6 ± 0.9 psu) to 316 mm H_2O year^{-1} in lower stands (at 3.0 ± 1.0 psu) at Strawberry Swamp (Table 4). This influence is based solely on *dbh*-dependent modeling of stand water use. Individual plots ($N = 2$ per location) in middle and lower stand locations differed in this estimation by 73 and 112 mm H_2O year^{-1} between them, respectively, reflecting the high forest structural variability at these locations along the salinity gradient. The more saline stands had lower leaf area index (LAI) as determined using an LAI-2000 approach (Li-Cor Environmental, Inc., Lincoln, NE, USA) with an 84° view angle, which ranged from 3.8 in the freshest zones ($n = 15$) to 2.1 in the more saline zones ($n = 9$). This is more reflective of overstory canopy openness of taller trees than mid-story species ingrowth at higher salinities and sunlight. In middle and lower stands the evergreen trees accounted for 1.7–6.4% of stand water use, respectively, versus <1.2% in freshwater, reflecting the greater contributions of larger waxmyrtle (*dbh* ≥ 10 cm) as forest structure changed in response to increased salinity. Nonetheless, these larger fractions of transpiration by evergreen shrubs do not offset the apparently lower transpiration by canopy trees in the lower and middle stands, and thus their stand water use is smaller than those of the freshwater stands.

Sap flow attenuation with radial depth into the sapwood of trees along the Strawberry Swamp salinity gradient also varied significantly by salinity ($F_{1,66} = 5.20$; $P = 0.0259$) and by species ($F_{2,66} = 9.76$; $P = 0.0002$); the interaction term, however, was not statistically significant (salinity × species; $P > 0.05$) (Fig. 2). This means that not only do tree size distributions change along the salinity gradient, but also do the functions describing the radial attenuation of sapflow in similarly sized trees, with consistency among the species despite any visual disparity for waxmyrtle (Fig. 2).

An important driver of stand water use change was a concomitant reduction in individual tree water use from 75 to 26 L H_2O day^{-1} for water tupelo and swamp tupelo in upper freshwater versus lower stands

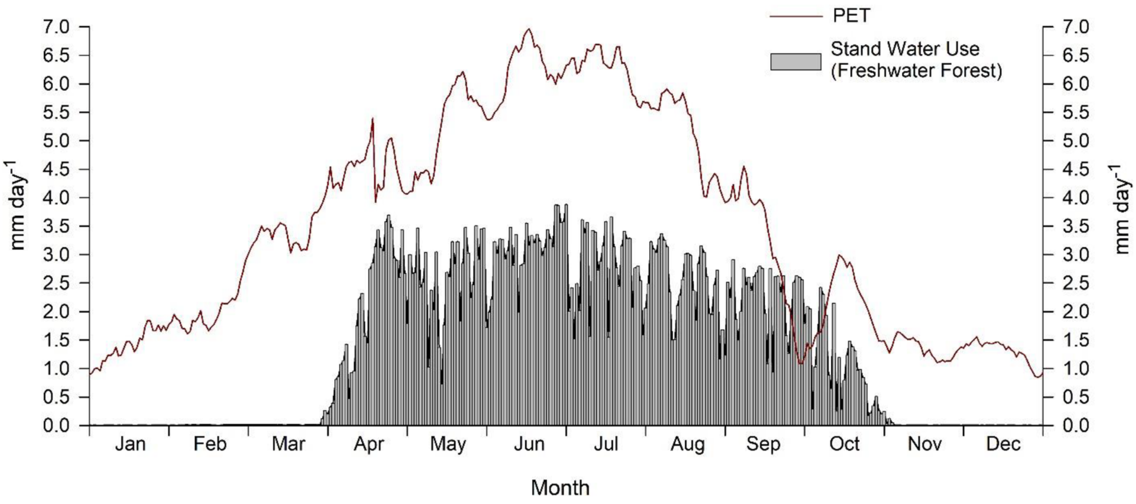

Fig. 4. Stand water use (mm H_2O day^{-1}), as an average of the two freshwater stands at Strawberry Swamp, Hobcaw Barony, South Carolina, USA for 2015/2016, versus estimated potential evapotranspiration (PET, mm H_2O day^{-1}, 7-day running average), assumed to be equal to PET derived using the Priestley-Taylor Method. Both were determined through modeling linked to environmental variables. Environmental data from January to mid-April are from 2016, and the remainder of the data in this graph are from 2015 because data were missing over those months in 2016 (location of environmental data collection depicted by the cross symbol, Fig. 1).

Table 4
Stand water use (mm H_2O year^{-1}) and the relative influences of forest structural effects alone, salinity effects alone, and forest structural and salinity effects in combination at Strawberry Swamp, Hobcaw Barony, South Carolina, USA.

		Forest structural effects				Salinity effects[a]		Forest structural × Salinity effects	
Stand	Plot	Evergreen	Deciduous	By Plot	Sub-total	By Plot	Sub-total	By Plot	Total
Upper	1	3.3	494.3	497.6	493.7	497.6	493.7	497.6	493.7
	2	5.7	484.1	489.8		489.8		489.8	
Middle	1	6.0	348.9	354.9	392.7	325.5	323.0	232.2	256.9
	2	8.6	421.8	430.4		320.4		281.6	
Lower	1	17.0	248.5	265.5	316.1	299.1	296.7	159.6	190.0
	2	6.3	360.4	366.7		294.4		220.4	

[a] Salinity was 0.7, 2.6, and 3.0 psu at Upper, Middle, and Lower stands, respectively.

with higher salinity (Fig. 5A). Water use per unit diameter ranged from only 0.9 to 1.2 L H_20 day^{-1} cm^{-1} in baldcypress along the salinity gradient (Fig. 5B). In contrast, water and swamp tupelo decreased unit-diameter water use rates from 2.5 to 1.2 L H_20 day^{-1} cm^{-1} in response to salinity. These are low rates (Lovelock et al., 2016), further highlighting the potential for a pervasive influence of salinity on the physiology of normally freshwater wetland forests, especially for the more salt-sensitive *Nyssa* spp.

The influence of salinity on radial patterning of sap flow (i.e., the eco-physiological effects of salinity) reduces middle and lower stand water use by an additional 66 and 107 mm H_2O year^{-1}, respectively, relative to freshwater stands. The result is that the combined effect of forest structural changes and tree eco-physiological adjustments to salinity depresses stand water use from 494 mm H_2O year^{-1} in freshwater settings to 257 and 190 mm H_2O year^{-1} in the progressively higher salinities of the middle and lower stands (Table 4). This is equal to reductions in stand water use by 48% at 2.6 psu salinity and 61% at 3.0 psu.

4. Discussion

4.1. Salinity and forest structure

Reduction in sap flow along the Strawberry Swamp salinity gradient for baldcypress and water tupelo followed reductions in transpiration from salinity observed in controlled settings. When viewed as a percentage of sap flow under freshwater conditions, the sap flow capacity of baldcypress and water tupelo is reduced by approximately 7% and 38%, respectively, per unit increase in salinity (psu) (Fig. 6). This response compares to the greenhouse literature available on baldcypress and water tupelo (Pezeshki, 1990; Pezeshki et al., 1986, 1987, 1988, 1989, 1995; Javanshir and Ewel, 1993; McLeod et al., 1996; Allen et al., 1997; Krauss et al., 2009a), which indicates that the transpirational capacity for these species would decrease by approximately 10% per psu increase in salinity. Comparisons between trees and seedlings are closer for baldcypress than for water tupelo, suggesting that more studies should be conducted on mature trees in the field if we are to understand how changes in salinity affect real wetland forests. In fact, the reviewed greenhouse studies were conducted on young seedlings over short time frames (generally < 90 day, with some exception), and the controlled nature and short duration of these studies omit long-term susceptibility stresses such as changes in osmotic stress potential and accumulation of sulfides in porewater. Furthermore, studies that focus on baldcypress seedings impose salinity up to 10 psu. We limited our literature summary to 8 psu (Fig. 6), but the field distribution of mature baldcypress is generally restricted to 3-4 psu as a mean long-term salinity condition (Harlow and Harrar, 1969; Chabreck, 1972; Krauss et al., 2017), which is enough to cause mortality in drier years (Cormier et al., 2013). Seedling studies on water tupelo routinely use salinities up to 3 psu, which better approximates typical field values (up to just 2.1 psu for water tupelo in Strawberry Swamp). We have less insight for waxmyrtle and swamp tupelo, but they seem to be restricted

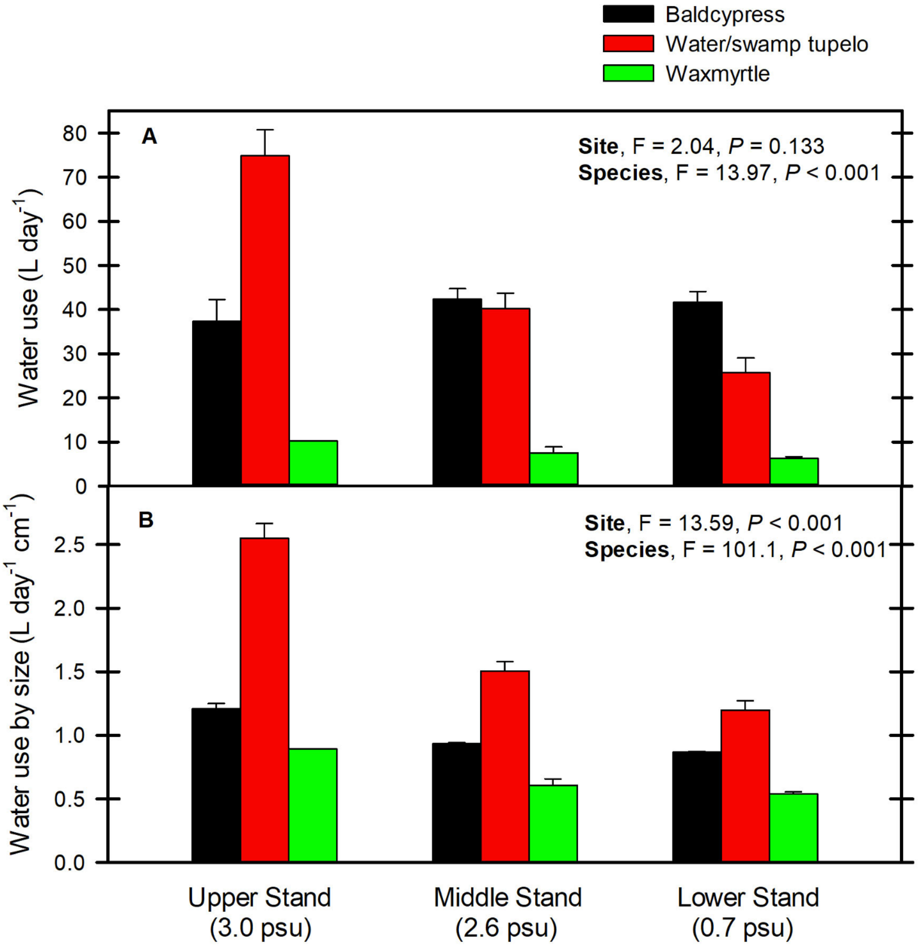

Fig. 5. (A) Individual tree water use (as maximum calculated L H_2O day^{-1}) and (B) water use by *dbh* (L H_2O day^{-1} cm^{-1}) for dominant and co-dominant crown class baldcypress (average *dbh* 42.4 ± 2.3 cm) and water tupelo/swamp tupelo (average *dbh* 35.2 ± 2.0 cm), and intermediate crown class waxmyrtle (average *dbh* 11.9 ± 1.0 cm) trees associated with a salinity gradient at Strawberry Swamp, Hobcaw Barony, South Carolina, USA. Salinity was 0.7, 2.6, and 3.0 psu at Upper, Middle, and Lower stands, respectively.

naturally to salinities below ~2 psu (Chabreck, 1972; Krauss et al., 2009b). The performance of waxmyrtle at salinities above 2.5 psu under high light levels at Strawberry Swamp is intriguing. The salinity tolerance of waxmyrtle might be higher than we currently recognize, and the increasingly patchy canopy in higher salinity zones may provide for a more favorable light environment that offsets the less favorable salinity.

Curiously, total basal area did not change much along the salinity gradient at Strawberry Swamp (Table 1). Rather, the upper stands had a greater density of smaller trees of all co-occurring species than middle and lower stands, which translates to higher stand water use in the model because the fraction of sapwood area per basal area is generally higher in smaller or younger trees (e.g., in baldcypress: Allen et al., 2015). The presence of larger baldcypress trees relative to the other species in our middle and lower stands indicates that these trees likely grew for many years before salinity impacted the site, and the stand consists of relict individual trees that developed previously in fresher water. This is not uncommon at sub-lethal salinities in the Southeastern U.S.; conversion from wetland forests to marsh is often projected to occur around 2 psu (Hackney et al., 2007), but this conversion can take many decades even with persistent salinization. In contrast, water tupelo, swamp tupelo, and ash are all smaller in middle and/or lower sites than upper sites at Strawberry Swamp and likely reflect more recent development than the baldcypress. Many baldcypress on Hobcaw Barony date back to the late 1700s (Krauss and Duberstein, 2010). Thus, as larger baldcypress trees become progressively stressed with salinity intrusion over the years, individual tree leaf area decreases from persistent lack of vascular support stemming from osmotic stress, which reduces crown area (Krauss and Duberstein, 2010). Baldcypress and water tupelo trees with persistent dieback and epicormic branching are common in middle and lower sites at Strawberry Swamp. Since *dbh* reflects decades (or centuries) of prior growth, whereas tree leaf areas reflect instantaneous or recent growing conditions, the two metrics can become disjointed in stressed forests. While compensatory increases in transpiration by residual leaves can hypothetically occur, as observed with shifts in leaf-to-sapwood area after wind disturbance events (Oren et al., 1999), this was not the case here because the water use of the relict large baldcypress trees was much less than that of the densely stocked smaller trees in the freshwater sites.

Visual evidence of the stands in Strawberry Swamp suggests that these tree species root into soil depths below floodwaters, and thus are likely to be rooted deeper than terrestrial forests where the most active roots are often within 23 cm of the soil surface (Schenk and Jackson, 2002). Deeper salinity concentrations at 60-100 cm depths were slightly better correlated with sap flow responses of all species at Strawberry Swamp than shallower observations. Often, salinity concentrations increase with sampling depth into the soil in coastal wetland forests (Marchand et al., 2004; Hsueh et al., 2016), as it did at Strawberry Swamp, but it is also very common to limit porewater sampling to less than 50 cm in many studies. If roots are active at depths that we ignore, and those depths are typically more saline, then past studies may systematically under-estimate tree tolerance to salinity

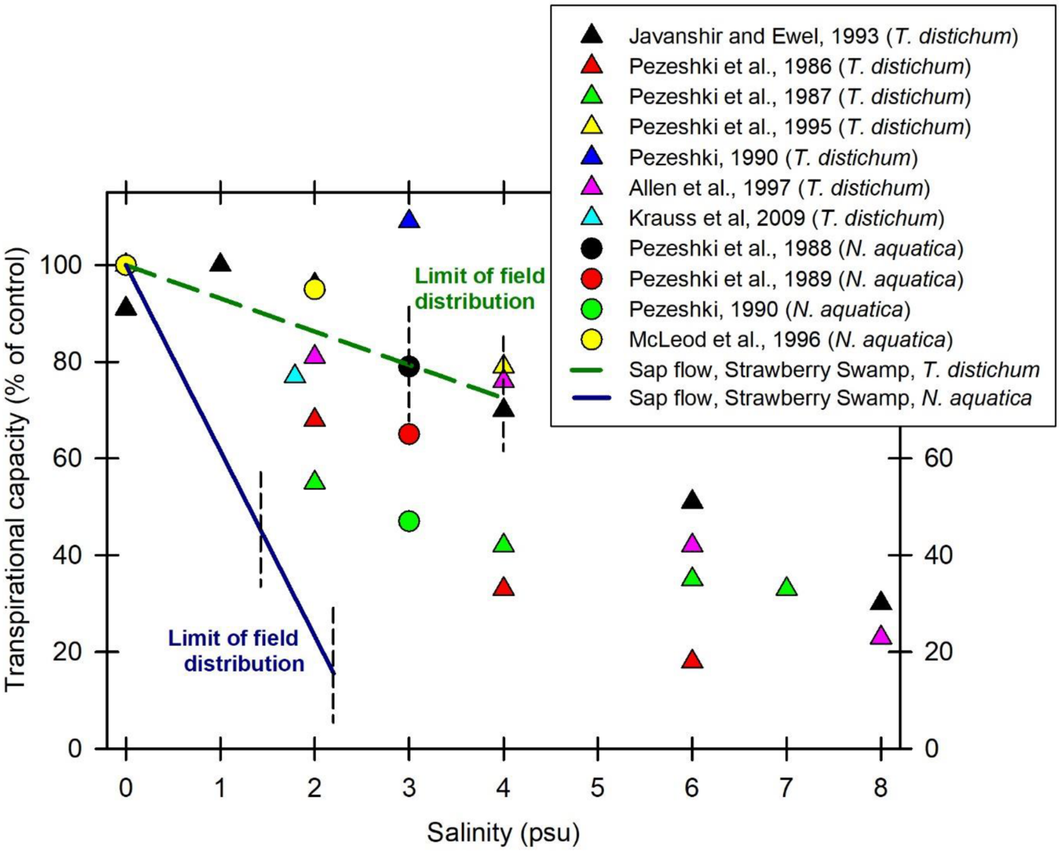

Fig. 6. Salinity-induced reductions in transpiration relative to values observed in fresh water, inferred from previously reported stomatal conductance data (greenhouse studies) and sap flow data from this study (field study). The regressions represent baldcypress (green) and water tupelo (black) from Strawberry Swamp, with their associated range of projected field distributions also depicted. (For interpretation of the references to color in this figure legend, the reader is referred to the web version of this article.)

in field setting.

It is also possible that the trees in Strawberry Swamp are more dependent on water extraction from deeper depths where porewater chemistry might be less variable; however, this may preclude opportunistic water uptake from pulses of rain water that would incorporate into the upper porewater and surface layers first. It is unlikely that trees would fail to use this fresh water. Hsueh et al. (2016) discovered preferential water uptake from the vadose zone (hummock soils above the water table) versus more salinized surface waters for baldcypress growing on hummocks in a Louisiana, USA, coastal wetland forest, and Zhai et al. (2018) found that baldcypress growing along the Waccamaw River, South Carolina, USA, preferentially use fresh surface water that is isotopically enriched by evaporation on some sites while waxmyrtle tended to use water below the soil surface. For our study, what is most important is that salinity measurements and sap flow were coupled across the salinity gradient for all species, allowing predictions of water use along our hypothesized gradient of influence.

4.2. Radial depth profiles

The presence of salinity interferes with xylem tensions from increased osmotic potential of soil waters (and thus leaf area support), which can lead to severe declines in water use of trees both by sap flow reductions (Stiller, 2009), and by variability in radial sap flow reductions across the sapwood (Krauss and Duberstein, 2010). Indeed, basal area growth per unit sapwood area was appreciably lower for salinized wetland forest sites in Louisiana, USA, than for freshwater wetland forest sites (Allen et al., 2019). With progressive salinization, tracheids associated with outer sapwood in baldcypress have more Na^+ and Cl^- ions than inner tracheids (Yanosky et al., 1995) and deeper radial depths may have higher concentrations of compatible solutes (e.g., methyl proline) for osmotic regulation (Carter et al., 2006b), both of which can slow sap flow. Radial patterning of sap flow has been best characterized for a many species of trees, both ring porous and diffuse porous, by using exponential decline functions (e.g., Berdanier et al., 2016). Similarly, Krauss and Duberstein (2010) fit radial attenuation curves for baldcypress in the nearby Reserve Swamp using an exponential decline function for salt-impacted trees, and a combination of linear and exponential decline for trees in freshwater conditions. Inverse first order polynomial regressions of our salinity-adjusted multipliers (which include factors of salinity and forest structure; Fig. 3) versus radial depth into the sapwood also had high coefficients of determination at all salinity levels for baldcypress ($r^2 \geq 0.92$), water tupelo ($r^2 \geq 0.77$), and swamp tupelo ($r^2 \geq 0.85$). We saw no evidence that the radial pattern in waxmyrtle sap flow was affected significantly by salinity (Table 3), but fewer observations were available for waxmyrtle so salinity effects may have been confounded by the aforementioned higher incident light levels at higher salinities as waxmyrtle transitioned from suppressed to co-dominant.

Krauss and Duberstein (2010) discovered that salinity-forced acute suppression of sap flow radially from sapwood depths of 15 mm to 25 mm in baldcypress trees from Reserve Swamp is remarkably similar to what we found for freshwater sites at Strawberry Swamp. Constraining the radial variability in sap flow response is an inherent challenge with these techniques, including even having to sort diurnal and seasonal shifts in radial sap flow patterns in some forest tree species (Ford et al., 2004). In all, overall sap flow rates at Strawberry Swamp were within the range previously reported for baldcypress trees in other

South Carolina sites (35.9 g H_2O m^{-2} s^{-1} at Strawberry Swamp vs. 30.1–43.0 g H_2O m^{-2} s^{-1} in Krauss and Duberstein, 2010) but ranges were quite different than previously used in stand water use modeling for water and swamp tupelo (46.0–86.3 g H_2O m^{-2} s^{-1} at Strawberry Swamp vs. 51.7 g H_2O m^{-2} s^{-1} in Krauss et al., 2015a). These average rates are indeed difficult to quantitatively compare because of the overwhelming tree-to-tree variation, nonetheless, salinity appears to relatively consistently reduce sap flow in these freshwater wetland trees.

With the exception of one waxmyrtle tree (*dbh* 7.7 cm; see Table S1, Appendix A), we did not assess trees <10 cm *dbh*, though the contributions of mid-story evergreen shrubs were probably important even though only ~4 mm H_2O $year^{-1}$ (e.g., less than some daily water use observations; Fig. 4). Understory woody vegetation can make important contributions to stand water use (Kelliher et al. 1998; Wullschleger et al., 2001; Oishi et al., 2008), and at Strawberry Swamp, the contribution of the waxmyrtle shrub layer that is taller than 1.3 m but with average *dbh* 11.9 ± 1.0 cm, may be substantial. Small waxmyrtle density increased from 4,950 individuals ha^{-1} in the upper freshwater stands to 8,680 and 8,550 individuals ha^{-1} in the middle and lower stands, respectively, with most of these shrubs occurring within the smaller diameter classes not included in our stand water use calculations (Liu et al., 2017). With our approach, we assume that most waxmyrtle-associated differences in water use occur after growth to ≥10 cm *dbh* size classes.

4.3. *Stand water use*

Stand water use in the flooded freshwater wetland forests of Strawberry Swamp was estimated to be approximately 39% of PET on an annual basis, and 49% during the growing season, for our composite study years of 2015/2016 (Fig. 4). Stand water use of 494 mm H_2O $year^{-1}$ is not especially high; for example, it only slightly exceeds values for hardwood forest stands in much more northern latitudes in Europe (151–407 mm H_2O $year^{-1}$, and coniferous forest stand water use of 279–427 mm H_2O $year^{-1}$; Roberts, 1999). However, our estimated rates of stand water use are within the range of values observed in other southeastern wetland forests: 350–872 mm H_2O $year^{-1}$ (Krauss et al., 2015a, 2015b). While some small errors may result from using standard TDP calibrations (Granier, 1987), usually only a small fraction of the TDP errors is attributable to calibration performance (Flo et al., 2019). Furthermore, we focus mostly on changes along the salinity gradient that might drive relative differences in water use patterns; however, it should be noted that values of 494, 257, and 190 mm H_2O $year^{-1}$ for the upper, middle, and lower sites are intended to be representative calculations of true stand water use and can be reestablished if TDP calibrations for these probes are altered for these species in course. It was also beyond the scope of our study to include understory transpiration (and evaporation), which is perhaps why transpiration was estimated to be about 59% of ET in a North Carolina hardwood forest (Oishi et al., 2008), versus our 39–49%.

Salinity was projected to reduce stand water use from 660 mm H_2O $year^{-1}$ to 164 mm H_2O $year^{-1}$ for a different salinized watershed in South Carolina, USA (Reserve Swamp: Krauss et al., 2015a). The drought conditions prevailing prior to and during that study resulted in salinity levels of 5.5 psu (compared to a previous running average of 1.3 psu), and stand water use was 25% of the stand water use of a nearby freshwater control site. At Strawberry Swamp stand water use at the highest salinity of 3 psu was 38% of stand water use in freshwater stands. Re-calculating this for Strawberry Swamp for a salinity of 5 psu adjusts this percentage to 21%, suggesting fairly strong convergence in salinity influences between these two studies in a relative sense, even though they were based on different approaches (gradient versus comparative) and had slightly different radial patterns of sap flow response.

Herein, we focused on reductions in stand water use from the perspective of forest vegetation, although these sites will become increasingly dominated by marsh grasses and understory shrubs (e.g., waxmyrtle, dahoon) as the canopy degrades and transmits more light to the understory. In this situation, compensatory water use of the released mid-story and understory need to be considered. Although waxmyrtle stem density nearly doubled, the LAI in the more saline stands was lower than that of the freshest zones, reflecting the sparse overstory canopy in saline zones. Accordingly, waxmyrtle sap flow at a radial depth of 15 mm increased by 63% coincident with this gradient in light availability, even when considering trees ≥10 cm *dbh* only, versus all stems. Nevertheless, it was visually obvious that a significant fraction of total leaf area in saline zones is attributable to waxmyrtle, which had relatively small water use per individual (Fig. 5A). Furthermore, *Phragmites australis* is also encroaching inland from areas downgradient (and more saline) of the waxmyrtle. *Phragmites* is an invasive reed that tolerates salinity and can use water vigorously (Burba et al., 1999; Herbst and Kappen, 1999). Understanding the ecohydrological consequences of these forest-to-marsh vegetation shifts with salinization will ultimately require consideration of all vegetation components.

5. Management implications and conclusions

In this study, we found that both salinity-induced changes in forest structure and changes in individual tree physiology occurred along a salinity gradient. Across salinity concentrations ranging from fresh to 3 psu, forest structural changes alone resulted in stand water use reductions from 494 mm $year^{-1}$ in freshwater stands to 316 mm $year^{-1}$ in stands of higher salinity. Changes in tree function (inferred from radial sap flux profiles) also occurred along this gradient, as sap flow rates decreased by an additional 13.3% per unit increase in salinity (psu) independently of forest structural changes on water use. Consequently, stand water use was estimated to be only 190 mm $year^{-1}$ in higher saline settings. Thus, our results demonstrate that the effects of salinization on transpiration cannot be predicted by changes in forest structure alone. Instead, estimates and model representations should also account for salinity's effects on the radial profile of sap flow, which results in reduced water fluxes.

Sea level rise is occurring and will continue to accelerate into the future. As a result, saltwater intrusion has become a primary stressor in many coastal wetland systems (White and Kaplan, 2017). The impacts of saltwater intrusion on coastal wetlands can vary depending on the magnitude, duration, and frequency of saltwater intrusion into the wetland. An early sign of salinity stress in trees is reduced sap flow as seen in this study where sap flow rates decreased by an additional 13.3% per unit increase in salinity (psu). We also know that net primary productivity can be twice as high in forests with low salinity relative to those with high salinity (Pierfelice et al., 2017). In the long-term, increased salinity levels leads to tree mortality and can cause large shifts in vegetation community composition (Kaplan et al. 2010), with invasive species likely to expand their ranges into coastal areas (Tully et al., 2019). Craft et al. (2009), using the maximum IPCC sea level rise scenario, estimated that Georgia tidal freshwater swamps will decline in areal extent by as much as 34%. It is only through studies like this that we will begin to understand the complex ecological processes occurring in coastal wetlands and allow us to predict and manage changes in coastal systems as sea levels rise.

Credit authorship contribution statement

Jamie A. Duberstein: Conceptualization, Methodology, Software, Validation, Formal analysis, Investigation, Resources, Data curation, Writing - review & editing, Visualization, Project administration, Funding acquisition. **Ken W. Krauss:** Conceptualization, Methodology, Software, Validation, Formal analysis, Investigation, Resources, Data curation, Writing - original draft, Supervision, Project administration,

Funding acquisition. **Michael J. Baldwin:** Software, Formal analysis, Data curation, Visualization. **Scott T. Allen:** Conceptualization, Methodology, Formal analysis, Resources, Data curation, Writing - review & editing, Funding acquisition. **William H. Conner:** Conceptualization, Resources, Writing - review & editing, Supervision, Funding acquisition. **John S. Salter:** Investigation. **Michael Miloshis:** Conceptualization, Investigation.

Declaration of Competing Interest

The authors declare that they have no known competing financial interests or personal relationships that could have appeared to influence the work reported in this paper.

Acknowledgments

Funding for this study was provided by the U.S. Geological Survey, Land Change Science Research and Development Program, and represents collaboration with the U.S. Geological Survey, Water Availability and Use Science Program. WHC was also supported in part by the National Institute of Food and Agriculture, U.S. Department of Agriculture, under project number SC 1700531. This represents Technical Contribution No. 6690 of the Clemson University Experimental Station. We thank Paul Conrads (USGS South Atlantic Water Science Center) and Steven Hutchinson (Clemson University) for decades of natural resource investigations in the Carolinas and their encouragement to take on this coastal watershed study. We thank Darren Johnson for tremendous assistance with the statistical analyses detailed in this paper and James Landmeyer for reviewing a previous version of this manuscript. We also acknowledge the assistance of many Clemson University staff and technicians who made this study possible, including Dan Hitchcock, Ani Jayakaran, Jeff Vernon, Brian Williams, Bo Song, and Ryan Marsh. Finally, we thank the Baruch Foundation for allowing us access to multiple field sites included in this manuscript. Data generated during this study are available at https://doi.org/10.5066/P9IR2XUO (Duberstein et al., 2018). Any use of trade, firm, or product names is for descriptive purposes only and does not imply endorsement by the U.S. Government.

Appendix A. Supplementary material

Supplementary data to this article can be found online at https://doi.org/10.1016/j.foreco.2020.118308.

References

Allen, J.A., Chambers, J.L., Pezeshki, S.R., 1997. Effects of salinity on baldcypress seedlings: Physiological responses and their relation to salinity tolerance. Wetlands 17 (2), 310–320. https://doi.org/10.1007/BF03161419.

Allen, S.T., Whitsell, M.L., Keim, R.F., 2015. Leaf area allometrics and morphometrics in baldcypress. Can. J. For. Res. 45 (8), 963–969. https://doi.org/10.1139/cjfr-2015-0039.

Allen, S.T., Reba, M.L., Edwards, B.L., Keim, R.F., 2017. Evaporation and the subcanopy energy environment in a flooded forest. Hydrol. Process. 31 (16), 2860–2871. https://doi.org/10.1002/hyp.11227.

Allen, S.T., Keim, R.F., Dean, T.J., 2019. Contrasting effects of flooding on tree growth and stand density determine aboveground production, in baldcypress forests. For. Ecol. Manage. 432, 345–355. https://doi.org/10.1016/j.foreco.2018.09.041.

Berdanier, A.B., Miniat, C.F., Clark, J.S., 2016. Predictive models for radial sap flux variation in coniferous, diffuse-porous and ring-porous temperate trees. Tree Physiol. 36 (8), 932–941. https://doi.org/10.1093/treephys/tpw027.

Burba, G.G., Verma, S.B., Kim, J., 1999. Surface energy fluxes of *Phragmites australis* in a prairie wetland. Agric. For. Meteorol. 94 (1), 31–51. https://doi.org/10.1016/S0168-1923(99)00007-6.

Carter, J.L., Veneklaas, E.J., Colmer, T.D., Eastham, J., Hatton, T.J., 2006a. Contrasting water relations of three coastal tree species with different exposure to salinity. Physiol. Plant. 127 (3), 360–373. https://doi.org/10.1111/j.1399-3054.2006.00633.x.

Carter, J.L., Colmer, T.D., Veneklaas, E.J., 2006b. Variable tolerance of wetland tree species to combined salinity and water logging is related to regulation of ion uptake and production of organic solutes. New Phytol. 169 (1), 123–133. https://doi.org/10.1111/j.1469-8137.2005.01552.x.

Čermák, J., Cienciala, E., Kučera, J., Lindroth, A., Bednářová, E., 1995. Individual variation in sap-flow in large pine and spruce trees and stand transpiration: A pilot study at the central NOPEX site. J. Hydrol. 168 (1–4), 17–27. https://doi.org/10.1016/0022-1694(94)02657-W.

Chabreck, R.H., 1972. Vegetation, Water and Soil Characteristics of the Louisiana Coastal Region. Bulletin 664. Louisiana State University Agricultural Experiment Station, Baton Rouge, Louisiana. 72 p.

Clearwater, M.J., Meinzer, F.C., Andrade, J.L., Goldstein, G., Holbrook, N.M., 1999. Potential errors in measurement on nonuniform sap flow using heat dissipation probes. Tree Physiol. 19 (10), 681–687. https://doi.org/10.1093/treephys/19.10.681.

Conner, W.H., McLeod, K.W., McCarron, J.K., 1997. Flooding and salinity effects on growth and survival of four wetland species. Wetlands Ecol. Manage. 8 (2), 99–109. https://doi.org/10.1023/A:1008251127131.

Cormier, N., Krauss, K.W., Conner, W.H., 2013. Periodicity in stem growth and litterfall in tidal freshwater forested wetlands: Influences of salinity and drought in nitrogen recycling. Estuaries Coasts 36 (3), 533–546. https://doi.org/10.1007/s12237-012-9505-z.

Craft, C., Clough, J., Ehman, J., Joye, S., Park, R., Pennings, S., Guo, H., Machmuller, M., 2009. Forecasting the effects of accelerated sea-level rise on tidal marsh ecosystem services. Front. Ecol. Environ. 7, 73–79. https://doi.org/10.1890/070219.

Dawson, T.E., Burgess, S.S.O., Tu, K.P., Oliveira, R.S., Santiago, L.S., Fisher, J.B., et al., 2007. Nighttime transpiration in woody plants from contrasting ecosystems. Tree Physiol. 27 (4), 561–575. https://doi.org/10.1093/treephys/27.4.561.

Day Jr., J.W., Boesch, D.F., Clairain, E.J., Kemp, G.P., Laska, S.B., Mitsch, W.J., et al., 2007. Restoration of the Mississippi Delta: Lessons from Hurricanes Katrina and Rita. Science 315 (5819), 1679–1684. https://doi.org/10.1126/science.1137030.

De Bruin, H.A.R., Keijman, J.Q., 1979. The Priestley-Taylor evaporation model applied to a large, shallow lake in the Netherlands. J. Appl. Meteorol. 18 (7), 898–903. https://doi.org/10.1175/1520-0450(1979)018<0898:TPTEMA>2.0.CO;2.

Duberstein, J.A., Krauss, K.W., Conner, W.H., Bridges Jr., W.C., Shelburne, V.B., 2013. Do hummocks provide a physiological advantage to even the most flood tolerant of tidal freshwater trees? Wetlands 33 (3), 399–408. https://doi.org/10.1007/s13157-013-0397-x.

Duberstein, J.A., Krauss, K.W., Allen, S.T., Baldwin, M.J., 2018. Sap flow data from a long-hydroperiod forested wetland undergoing salinity intrusion in South Carolina, USA. USGS Data Release. https://doi.org/10.5066/P9IR2XUO.

Ellis, J.I., Schneider, D.C., 1997. Evaluation of a gradient sampling design for environmental impact assessment. Environ. Monit. Assess. 48 (2), 157–172. https://doi.org/10.1023/A:1005752603707.

Ericson, J.P., Vörösmarty, C.J., Dingman, S.L., Ward, L.G., Meybeck, M., 2006. Effective sea-level rise and deltas: Causes of change and human dimension implications. Global Planet. Change 50, 63–82. https://doi.org/10.1016/j.gloplacha.2005.07.004.

Flo, V., Martinez-Vilalta, J., Steppe, K., Schuldt, B., Poyatos, R., 2019. A synthesis of bias and uncertainty in sap flow methods. Agric. For. Meteorol. 271, 362–374. https://doi.org/10.1016/j.agrformet.2019.03.012.

Ford, C.R., Goranson, C.E., Mitchell, R.J., Will, R.E., Teskey, R.O., 2004. Diurnal and seasonal variability in the radial distribution of sap flow: Predicting total stem flow in *Pinus taeda* trees. Tree Physiol. 24 (9), 951–960. https://doi.org/10.1093/treephys/24.9.951.

Granier, A., 1987. Evaluation of transpiration in a Douglas-fir stand by means of sap flow measurements. Tree Physiol. 3 (4), 309–320. https://doi.org/10.1093/treephys/3.4.309.

Hackney, C.T., Avery, G.B., Leonard, L.A., Posey, M., Alphin, T., 2007. Biological, chemical, and physical characteristics of tidal freshwater swamp forests of the Lower Cape Fear River/Estuary, North Carolina. In: Ecology of Tidal Freshwater Forested Wetlands of the Southeastern United States. Springer, The Netherlands, pp. 183–221.

Harlow, W.M., Harrar, E.S., 1969. Textbook of Dendrology, fifth ed. MxGraw-Hill Book Company, New York.

Herbst, M., Kappen, L., 1999. The ratio of transpiration versus evaporation in a reed belt as influenced by weather conditions. Aquat. Bot. 63 (2), 113–125. https://doi.org/10.1016/S0304-3770(98)00112-0.

Hsueh, Y., Chambers, J.L., Krauss, K.W., Allen, S.T., Keim, R.F., 2016. Hydrologic exchanges and baldcypress water use on deltaic hummocks, Louisiana, USA. Ecohydrology 9 (8), 1452–1463. https://doi.org/10.1002/eco.1738.

James, S.A., Meinzer, M.C., Goldstein, G., Woodruff, D., Jones, T., Restom, T., et al., 2003. Axial and radial water transport and internal water storage in tropical forest canopy trees. Oecologia 134 (1), 37–45. https://doi.org/10.1007/s00442-002-1080-8.

Javanshir, K., Ewel, K., 1993. Salt resistance of bald cypress. In: Towards the Rationale Use of High Salinity Tolerant Plants. Kluwer, The Netherlands, pp. 285–291.

Jones, M.C., Bernhardt, C.E., Krauss, K.W., Noe, G.B., 2017. The impact of Late Holocene land use change, climate variability, and sea level rise on carbon storage in tidal freshwater wetlands on the Southeastern United States Coastal Plain. J. Geophys. Res. Biogeosci. 122 (12), 3126–3141. https://doi.org/10.1002/2017JG004015.

Kaplan, D., Munoz-Carpena, R., Ritter, A., 2010. Untangling complex shallow groundwater dynamics in the floodplain wetlands of a southeastern U.S. coastal river. Water Resour. Res. 46, W08528. https://doi.org/10.1029/2009WR009038.

Kelliher, F.M., Lloyd, J., Ameth, A., Byers, J.N., McSeveny, T.M., Milukova, I., et al., 1998. Evaporation from a central Siberian pine forest. J. Hydrol. 205 (3–4), 279–296. https://doi.org/10.1016/S0022-1694(98)00082-1.

Krauss, K.W., Duberstein, J.A., 2010. Sapflow and water use of freshwater wetland trees exposed to saltwater incursion in a tidally influenced South Carolina watershed. J. Coastal Res. 40 (3), 525–535. https://doi.org/10.1139/X09-204.

Krauss, K.W., Doyle, T.W., Howard, R.J., 2009a. Is there evidence of adaptation to tidal flooding in saplings of baldcypress subjected to different salinity regimes? Environ.

Exp. Bot. 67 (1), 118–126. https://doi.org/10.1016/j.envexpbot.2009.05.005.

Krauss, K.W., Duberstein, J.A., Doyle, T.W., Conner, W.H., Day, R.H., Inabinette, L.W., Whitbeck, J.L., 2009b. Site condition, structure, and growth of baldcypress along tidal/non-tidal salinity gradients. Wetlands 29 (2), 505–519. https://doi.org/10.1672/08-77.1.

Krauss, K.W., Duberstein, J.A., Conner, W.H., 2015a. Assessing stand water use in four coastal wetland forests using sapflow techniques: annual estimates, errors and associated uncertainties. Hydrol. Process. 29 (1), 112–127. https://doi.org/10.1002/hyp.10130.

Krauss, K.W., Barr, J.G., Engel, V., Fuentes, J.D., Wang, H., 2015b. Approximations of stand water use versus evapotranspiration from three mangrove forests in southeast Florida, USA. Agric. For. Meteorol. 213, 291–303. https://doi.org/10.1016/j.agrformet.2014.11.014.

Krauss, K.W., Shaffer, G.P., Keim, R.F., Chambers, J.L., Wood, W.B., Hartley, S.B., 2017. Performance Measures for a Mississippi River Reintroduction into the Forested Wetlands of Maurepas Swamp. Scientific Investigations Report 2017-5036 56 U.S. Geological Survey, Reston, Virginia. https://doi.org/10.3133/sir20175036.

Liu, X., Conner, W.H., Song, B., Jayakaran, A.D., 2017. Forest composition and growth in a freshwater forested wetland community across a salinity gradient in South Carolina, USA. For. Ecol. Manage. 389, 211–219. https://doi.org/10.1016/j.foreco.2016.12.022.

Lovelock, C.E., Krauss, K.W., Osland, M.J., Reef, R., Ball, M.C., 2016. The physiology of mangrove trees with changing climate. In: Tropical Tree Physiology: Adaptations and Responses in a Changing Environment. Springer, Switzerland. https://doi.org/10.1007/978-3-319-27422-5_7. p. 149467–179p.

Lu, P., Urban, L., Ping, Z., 2004. Granier's thermal dissipation probe (TDP) method for measuring sap flow in trees: Theory and practice. Acta Botanica Sinica 46 (6), 631–646.

Marchand, C., Baltzer, F., Lallier-Vergès, E., Albéric, P., 2004. Pore-water chemistry in mangrove sediments: Relationship with species composition and developmental stages (French Guiana). Mar. Geol. 208 (2–4), 361–381. https://doi.org/10.1016/j.margeo.2004.04.015.

McLaughlin, D.L., Brown, M.T., Cohen, M.J., 2012. The ecohydrology of a pioneer wetland species and a drastically altered landscape. Ecohydrology 5 (5), 656–667. https://doi.org/10.1002/eco.253.

McLeod, K.W., McCarron, J.K., Conner, W.H., 1996. Effects of flooding and salinity on photosynthesis and water relations of four Southeastern Coastal Plain forest species. Wetlands Ecol. Manage. 4 (1), 31–42. https://doi.org/10.1007/BF01876133.

Michener, W.K., Blood, E.R., Bildstein, K.L., Brinson, M.M., Gardner, L.R., 1997. Climate change, hurricanes and tropical storms, and rising sea level in coastal wetlands. Ecol. Appl. 7 (3), 770–801. https://doi.org/10.1890/1051-0761(1997)007[0770:CCHATS]2.0.CO;2.

Munns, R., Termaat, A., 1986. Whole-plant responses to salinity. Australian Journal of Plant Physiology 13 (1), 143–160. https://doi.org/10.1071/PP9860143.

Oishi, A.C., Oren, R., Stoy, P.C., 2008. Estimating components of forest evapotranspiration: A footprint approach for scaling sap flux measurements. Agric. For. Meteorol. 148 (11), 1719–1732. https://doi.org/10.1016/j.agrformet.2008.06.013.

Oren, R., Phillips, N., Ewers, B.E., Pataki, D.E., Megonigal, J.P., 1999. Sap-flux-scaled transpiration responses to light, vapor pressure deficit, and leaf area reduction in a flooded *Taxodium distichum* forest. Tree Physiol. 19 (6), 337–347. https://doi.org/10.1093/treephys/19.6.337.

Pezeshki, S.R., 1990. A comparative study of the responses of *Taxodium distichum* and *Nyssa aquatica* seedlings to soil anaerobiosis and salinity. For. Ecol. Manage. 33 (34), 531–541. https://doi.org/10.1016/0378-1127(90)90216-X.

Pezeshki, S.R., DeLaune, R.D., Patrick Jr., W.H., 1986. Gas exchange characteristics of bald cypress (*Taxodium distichum* L.): Evaluation of responses to leaf aging, flooding, and salinity. Can. J. For. Res. 16 (6), 1394–1397. https://doi.org/10.1139/x86-250.

Pezeshki, S.R., DeLaune, R.D., Patrick Jr., W.H., 1987. Response of baldcypress (*Taxodium distichum* L. var. *distichum*) to increases in flooding salinity in Louisiana's Mississippi River Deltaic Plain. Wetlands 7 (1), 1–10. https://doi.org/10.1007/BF03160798.

Pezeshki, S.R., DeLaune, R.D., Patrick Jr., W.H., 1988. Effect of salinity on leaf ionic content and photosynthesis of *Taxodium distichum* L. Am. Midland Natural. 119 (1), 185–192. https://doi.org/10.2307/2426067.

Pezeshki, S.R., Patrick Jr., W.H., DeLaune, R.D., Moser, E.D., 1989. Effects of waterlogging and salinity interactions on *Nyssa aquatica* seedlings. For. Ecol. Manage. 27 (1), 41–51. https://doi.org/10.1016/0378-1127(89)90081-9.

Pezeshki, S.R., DeLaune, R.D., Choi, H.S., 1995. Gas exchange and growth of bald cypress seedlings from selected U.S. Gulf Coast populations: Responses to elevated salinities. Can. J. For. Res. 25 (9), 1409–1415. https://doi.org/10.1139/x95-153.

Phillips, N., Oren, R., Zimmermann, R., 1996. Radial patterns of xylem sap flow in non-, diffuse- and ring-porous tree species. Plant, Cell Environ. 19 (8), 983–990. https://doi.org/10.1111/j.1365-3040.1996.tb00463.x.

Pierfelice, K.N., Lockaby, B.G., Krauss, K.W., Conner, W.H., Noe, G.B., Ricker, M.C., 2017. Salinity influences on above- and belowground net primary productivity in tidal wetlands. J. Hydrol. Eng. 22 (1), 5015002. https://doi.org/10.1061/(ASCE)HE.1943-5584.0001223.

Poyatos, R., Čermák, J., Llorens, P., 2007. Variation in the radial patterns of sap flux density in pubescent oak (*Quercus pubescens*) and its implications for tree and stand transpiration measurements. Tree Physiol. 27 (4), 537–548. https://doi.org/10.1093/treephys/27.4.537.

Priestley, C.H.B., Taylor, R.J., 1972. On the assessment of surface heat flux and evaporation using large-scale parameters. Mon. Weather Rev. 100 (2), 81–92. https://doi.org/10.1175/1520-0493(1972)100<0081:OTAOSH>2.3.CO;2.

Roberts, J., 1999. Plants and water in forests and woodlands. In Eco-hydrology: Plants and Water in Terrestrial and Aquatic Environments (pp. 181–236). Routledge, London and New York. 402 p.

Salinas, L.M., DeLaune, R.D., Patrick Jr., W.H., 1986. Changes occurring along a rapidly submerging coastal area: Louisiana, USA. J. Coastal Res. 2 (3), 269–284.

Schenk, H.J., Jackson, R.B., 2002. The global biogeography of roots. Ecol. Monogr. 72 (3), 311–328. https://doi.org/10.1890/0012-9615(2002)072[0311:TGBOR]2.0.CO;2.

Smith, H.R., 2012. In Land of Cypress and Pine: An Environmental History of the Santee Experimental Forest, 1683–1937. General Technical Report SRS-155. USDA Forest Service, Asheville, NC. 17 p.

Stiller, V., 2009. Soil salinity and drought alter wood density and vulnerability to xylem cavitation of baldcypress (*Taxodium distichum* (L.) Rich.) seedlings. Environ. Exp. Bot. 67 (1), 164–171. https://doi.org/10.1016/j.envexpbot.2009.03.012.

Stuckey, B.N., 1982. Soil Survey of Georgetown County, South Carolina. United States Department of Agriculture, Washington, D.C., pp. 97.

Tie, Q., Hu, H., Tian, F., Holbrook, N.M., 2018. Comparing different methods for determining forest evapotranspiration and its components at multiple temporal scales. Sci. Total Environ. 633, 12–29. https://doi.org/10.1016/j.scitotenv.2018.03.082.

Tully, K., Gedan, K., Epanchin-Niell, R., Strong, A., Bernhardt, E.S., Bendor, T., Mitchell, M., Kominski, J., Jordan, T.E., Neubauer, S.C., Weston, N.B., 2019. The invisible flood: The chemistry, ecology, and social implications of coastal saltwater intrusion. Bioscience 69 (5), 368–378. https://doi.org/10.1093/biosci/biz027.

White Jr., E., Kaplan, D., 2017. Restore or retreat? Saltwater intrusion and water management in coastal wetlands. Ecosyst. Health Sustain. 3 (1), e01258. https://doi.org/10.1002/ehs2.1258.

Van Doren, M. (Ed.), 1928. Travels of William Bartram. Dover Publications, Inc., New York. 414 p.

Williams, K., Ewel, K.C., Stumpf, R.P., Putz, F.E., Workman, T.W., 1999. Sea-level rise and coastal forest retreat on the west coast of Florida, USA. Ecology 80 (6), 2045–2063. https://doi.org/10.1890/0012-9658(1999)080[2045:SLRACF]2.0.CO;2.

Williams, T.M., Chow, A.T., Song, B., 2012. Historical visualization evidence on forest-salt marsh transition in Winyah Bay, South Carolina: a retrospective study in sea level rise. Wetland Sci. Pract. 29 (4), 5–17.

Wullschleger, S.D., Meinzer, F.C., Vertessy, R.A., 1998. A review of whole-plant water use studies in trees. Tree Physiol. 18 (8–9), 499–512. https://doi.org/10.1093/treephys/18.8-9.499.

Wullschleger, S.D., Hanson, P.J., Todd, D.E., 2001. Transpiration from a multi-species deciduous forest as estimated by xylem sap flow techniques. For. Ecol. Manage. 143 (1–3), 205–213. https://doi.org/10.1016/S0378-1127(00)00518-1.

Yanosky, T.M., Hupp, C.R., Hackney, C.T., 1995. Chloride concentrations in growth rings of *Taxodium distichum* in a saltwater-intruded estuary. Ecol. Appl. 5 (3), 785–792. https://doi.org/10.2307/1941986.

Zhai, L., Krauss, K.W., Liu, X., Duberstein, J.A., Conner, W.H., DeAngelis, D.L., Sternberg, L.D.S.L., 2018. Growth stress response to sea level rise in species with contrasting functional traits: A case study in tidal freshwater forested wetlands. Environ. Exp. Bot. 155, 378–386. https://doi.org/10.1016/j.envexpbot.2018.07.023.